CERN-ACC-2015-0215

EuCARD-2

Enhanced European Coordination for Accelerator Research & Development

Journal Publication

Laser fields in dynamically ionized plasma structures for coherent acceleration

Luu-Thanh, Ph. (Heinrich Heine Universität) *et al*

26 June 2016

The EuCARD-2 Enhanced European Coordination for Accelerator Research & Development project is co-funded by the partners and the European Commission under Capacities 7th Framework Programme, Grant Agreement 312453.

This work is part of EuCARD-2 Work Package **13: Novel Acceleration Techniques (ANAC2)**.

The electronic version of this EuCARD-2 Publication is available via the EuCARD-2 web site <http://eucard2.web.cern.ch/> or on the CERN Document Server at the following URL: <http://cds.cern.ch/search?p=CERN-ACC-2015-0215>

CERN-ACC-2015-0215

Eur. Phys. J. Special Topics **224**, 2625–2629 (2015)

DOI: 10.1140/epjst/e2015-02574-8

THE EUROPEAN PHYSICAL JOURNAL SPECIAL TOPICS

Review

Laser fields in dynamically ionized plasma structures for coherent acceleration

Ph. Luu-Thanh[1], T. Tückmantel[1], A. Pukhov[1,a], and I. Kostyukov[2,3]

[1] Theoretische Physik I, Heinrich Heine Universität, 40225 Dsseldorf, Germany
[2] University of Nizhny Novgorod, Nizhny Novgorod 603950, Russia
[3] Institute of Applied Physics RAS, Nizhny Novgorod 603950, Russia

Received 26 June 2014 / Received in final form 31 August 2015
Published online xx October 2015

Abstract. With the emergence of the CAN (Coherent Amplification Network) laser technology, a new scheme for direct particle acceleration in periodic plasma structures has been proposed. By using our full electromagnetic relativistic particle-in-cell (PIC) simulation code equipped with ionisation module, we simulate the laser fields dynamics in the periodic structures of different materials. We study how the dynamic ionization influences the field structure.

1 Introduction

With massive parallelism as its constitution concept, the concept for the Coherent Amplification Network (ICAN) involves a huge number of identical and mutually coherent laser pulses in a vast fibre array [1]. In the previous paper [2], we have proposed the non-resonating open periodic plasma structure for a particle accelerator that utilises the coherent laser field directly. A sketch of the plasma structure is shown in Fig. 1. One period of the whole scheme consists of two rectangular plasma slabs to screen the decelerating phase of the laser field. A hole with width w is drilled through the centre of the boxes along the x-axis to allow for electron beam propagation. The gap between two boxes is equal to half laser wavelength. A pair of counter-propagating laser beams, produced by the CAN technology, will interfere at the centre of the gap. If injected at a proper phase, an electron is able to harvest the accelerating field during the half laser period. The coherency of the laser beams provided by the CAN project allows us to construct a multitude of these structures.

Previously, it has been assumed that the whole structure has been pre-ionised. Thus, the effect of the ionisation process, which may strongly influence the evolution of the laser fields in the structure and later the particle beam propagation, has not been taken into account. In this paper, we study the interaction between the laser fields and the structure including dynamic field ionisation of the material. For the simulation model, we use the VLPL code [3] including the ionisation module. The effect of electron collisional-ionisations is neglected in our study since they are slow compared to the femtosecond pulse duration [4].

[a] e-mail: alexander.pukhov@tp1.uni-duesseldorf.de

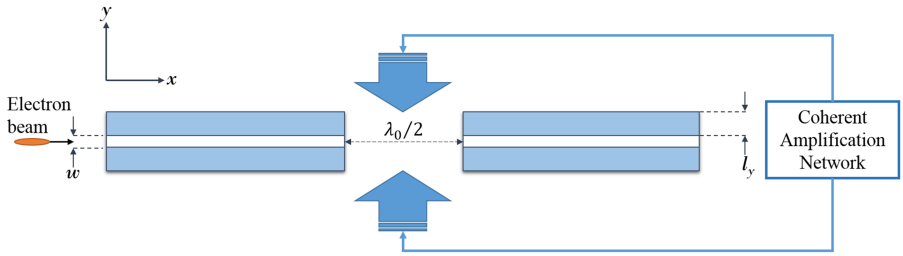

Fig. 1. Sketch of one period of the direct particle acceleration scheme using the CAN technology. Here, λ_0 is the laser wavelength, w is the hole width and l_y is the thickness of the structure. A pair of counter-propagating laser pulses is generated by the CAN system and interferes with each other at the centre of the structure. If injected at a proper phase, the electron beam will pick up the accelerating field in the cavity during half laser period and is screened from the decelerating field by the structure.

2 Method and Simulations

There are two limiting cases of ionisation: tunnelling ionisation ($\kappa \ll 1$) and multi-photon ionisation ($\kappa \gg 1$). Here, κ, introduced by Keldysh, is called the adiabaticity parameter and is defined as the ratio between the frequency of laser light ω and the frequency ω_t of electron tunnelling through an ionisation potential barrier of an atomic level U_{ion} [5],

$$\kappa = \frac{\omega}{\omega_t} = \omega \frac{\sqrt{2m_e U_{ion}}}{eE}, \tag{1}$$

in which E is the amplitude of the electric field, m_e and e are the electron mass and the elementary charge, respectively. At the early stage of the ionisation process, the ionisation potential U_{ion} of materials we study is from 20 eV to 120 eV and if the intensity of the laser field is about $I \approx 2 \times 10^{17}$ W/cm^2, eq. (1) yields $\kappa \approx 0.07$, which is in the applicable range of the tunnelling ionisation model. In our simulations, the time step Δt is smaller than the laser period T_0 ($\Delta t/T_0 = 0.005$), hence the laser field can be considered to be static in each time step. The tunnelling ionisation rate of complex atoms in a static field E is given by [6]

$$\begin{aligned} W_{DClm} &= \omega_a C^2_{n^*l^*} \frac{(2l+1)(l+|m|)!}{2^{|m|}(|m|)!(l-|m|)!} \times \left(\frac{U_{ion}}{2U_H}\right) \left[2\frac{E_a}{E}\left(\frac{U_{ion}}{U_H}\right)^{3/2}\right]^{2n^*-|m|-1} \\ &\times \exp\left[-\frac{2}{3}\frac{E_a}{E}\left(\frac{U_{ion}}{U_H}\right)^{3/2}\right]. \end{aligned} \tag{2}$$

Here, $U_H = 13.6$ eV is Hydrogen's ionisation potential at the ground state; $\omega_a = \alpha^3 c/r_e$ is the atomic unit frequency and $E_a = \alpha^4 m_e c^2/e r_e$, with α and r_e are the fine structure constant and classical electron radius, respectively; l and m are the electron's quantum number and its projection; $n^* = Z\sqrt{U_H/U_{ion}}$ is the effective principal quantum number and n_0^* is the value for the ground state; $l^* = n_0^* - 1$ is the effective value of the orbital number; Z is the ion charge number after ionisation. The coefficients $C_{n^*l^*}$, based on the Ammosov-Delone-Krainov (ADK) model [7], are

$$C^2_{n^*l^*} = \frac{2^{2n^*}}{n^*\Gamma(n^*+l^*+1)\Gamma(n^*-l^*)}. \tag{3}$$

Table 1. Properties of materials being used in our simulations. Note: The unit of atomic weight is in gram and the atom density is measured in term of plasma critical density $n_{cr} = \frac{\pi}{r_e \lambda_0^2}$, with r_e is the classical electron radius and λ_0 is the wavelength of a laser. For $\lambda_0 = 800$ nm, $n_{cr} \approx 1.742 \times 10^{21}$ cm^{-3}.

	Graphene	Aluminium	Copper
Element	C	Al	Cu
Atomic number	6	13	29
Atomic weight	12.011	26.982	63.546
Atom density	65.251	34.595	48.745
Electron configuration	[He]$2s^2 2p^2$	[He]$3s^2 3p^1$	[Ar]$3d^{10} 4s^1$

We study the stability of the accelerating field in periodic structures made out of three different materials: graphene, aluminium or copper. Table 1 shows the fundamental properties of these materials. Copper and aluminium atoms have 1 and 3 electrons in the outer shell, respectively. These are the electrons they contribute to the conduction band. For graphene, due to the hybridisation bonding, it has 1 electron available for the electronic conduction while the other 3 electrons are reserved for chemical bonding.

In our PIC simulations, the laser wavelength is assumed to be $\lambda_0 = 800$ nm. The periodic structure is sketched in fig. 1. The thickness of the structure is $l_y = 0.25\lambda_0$ and the width of the hole is $w = 0.2\lambda_0$. The ground state of the structure is simulated by seeding two species, ion and electron, into the simulation box at the beginning. The ion density is set equal to the atom density (see table 1) and the electron density is equal to the number of electrons in the conduction band multiplied by the atom density. Consequently, the ion species has initially the charge state corresponding to the number of electrons in the conduction band. The two counter-propagating laser pulses have Gaussian focal spots in the longitudinal direction (x) and their optical axes pass the centre of the structure. To save the computation time, we have chosen the beam diameter at the focal point $d = 3\lambda_0$ and the duration $\tau = 4\lambda_0/c$ for both pulses. The relativistically normalised laser amplitude is $a_L = eE_L/m_e\omega_0 c = 0.3$ that corresponds to an optical intensity $I \approx 1.924 \times 10^{17}$ W/cm^2. Here, E_L is the laser electric field amplitude, ω_0 is the laser frequency, m_e, e and c are the electron mass, the electron charge and the speed of light, respectively.

We use two dimensional planar geometry in our simulations. The simulation box is $7\lambda_0 \times 4\lambda_0$ with grid steps $0.01\lambda_0 \times 0.01\lambda_0$ in X, and Y directions. We use 8 particles per cell for each species. Figure 2 shows the simulation results for graphene, aluminium, and copper, respectively to each column. The pictures are taken at the simulation time $t = 6.4\lambda_0/c$. It can be clearly seen from the pictures that the dynamic ionisation process is very non-uniform in graphene and in copper structures. This leads to a significant disturbance of the fields in the cavity and inside the hole. In contrast, in aluminium structures at the same time of simulation, the ionisation process only starts occurring at the edges of the structure while the integrity of the field in the cavity is still robustly maintained.

With aluminium's coming up as the potential material for the structure, we also test the dependence of the field on the hole width w, while keeping other simulation parameters intact. We run a set of simulations with the hole widths $d_{\text{hole}} = \{0.1\lambda_0, 0.2\lambda_0, 0.3\lambda_0, 0.4\lambda_0\}$. Figure 3 shows the simulation results. Similarly, the pictures are taken at the simulation time $t = 6.4\lambda_0/c$. Upon observing the pictures we notice that as the width increases the shape of the electric field at the centre of the structure changes from a flat-top into a bell-like shape. Moreover, the results also tell us that with the increase of the width, the shielding is losing its effectiveness by

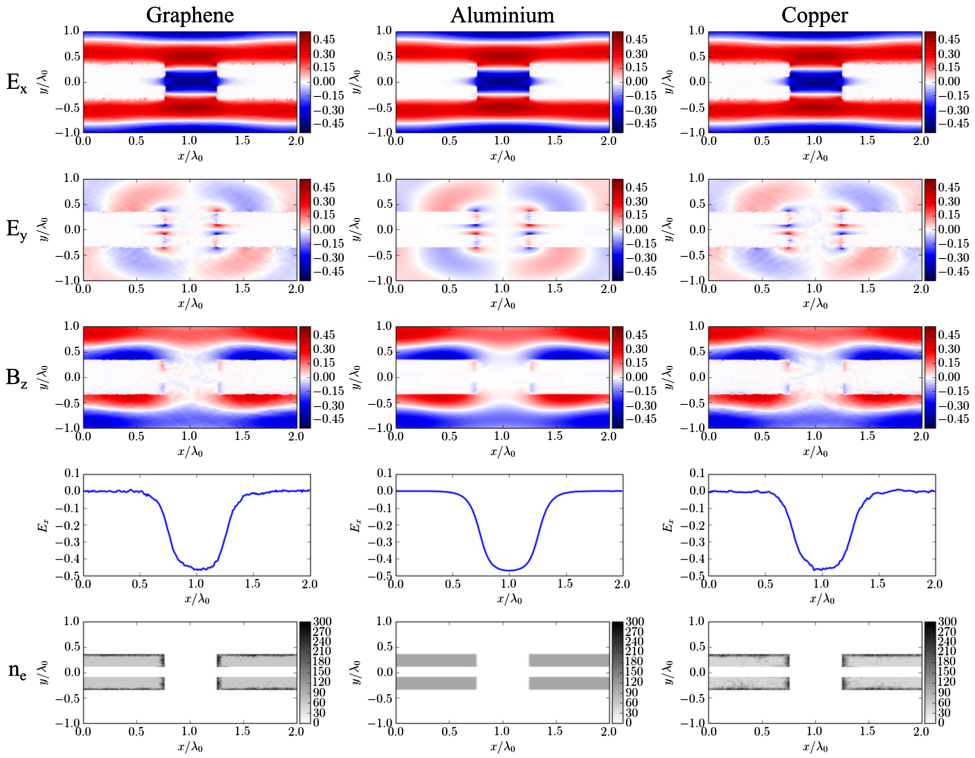

Fig. 2. Results of simulations modelling the interaction between a pair of counter-propagating laser pulses and the structure. The materials being used are graphene, aluminium and copper, corresponding for each column. The first three rows illustrate the longitudinal E_x, transversal E_y fields, and the magnetic field B_z, respectively. The fourth row shows the one-dimensional cut of the electric field E_x at the centre of the structure along the x-axis. The last row depicts the electron density of the structure.

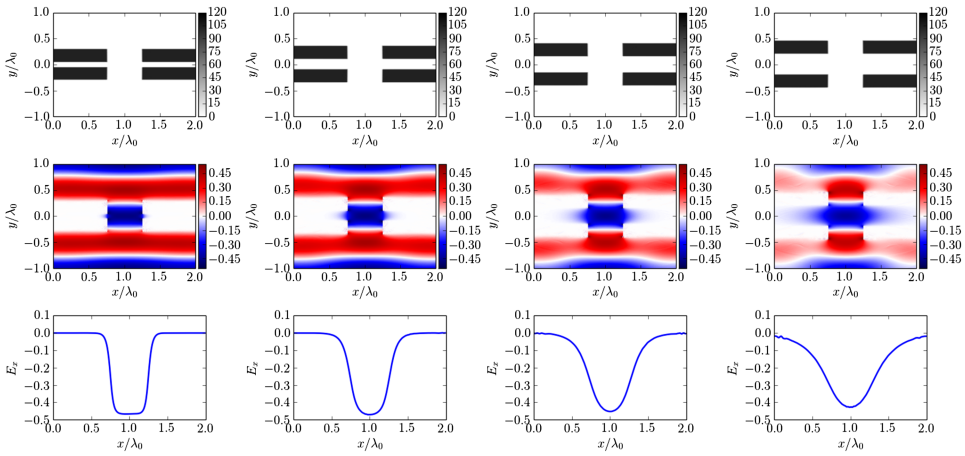

Fig. 3. Simulation results of aluminium with different hole sizes w. Aluminium is used as the material for every simulation. The width is $0.1\lambda_0$, $0.2\lambda_0$, $0.3\lambda_0$ and $0.4\lambda_0$ from left to right, respectively. The first row shows the normalised electron density n_e/n_{cr} of the structure. The middle rows depicts the normalised electric field E_x. The bottom row plots the 1D cut of the longitudinal electric field E_x at the centre of the structure along the x-axis.

letting more field tunnelling into the hole, which is not desired for particle acceleration. We also note that for the wider hole, the peak of the field amplitude is smaller. Thus, by keeping the width $w \leq 0.2\lambda_0$ the structure can shield off the field effectively and produce a decent field for particle acceleration.

3 Summary

To conclude, we have studied the evolution of laser fields in the periodic structure with three different materials: graphene, aluminium, and copper. Due to the ionisation process, a strong disturbance occurs in structures made of graphene and copper, which renders these materials unsuitable for our scheme of particle acceleration. Meanwhile, the robustness of aluminium allows us to produce a decent field, which can be used to accelerate particles. Moreover, the shape and the peak of the field amplitude are also influenced by the width of the hole. By maintaining the width $w \leq 0.2\lambda_0$, the field achieves the higher amplitude and has a flat-top profile. Our next step is to study the injection and particle dynamics of electron beams in the structure. These tasks will be discussed in our future publication.

This work has been supported in parts by the Government of the Russian Federation (Project No. 14.B25.31.0008) and by the Russian Foundation for Basic Research (Grants Nos. 13-02-00886), by EU FP7 EUCARD2, and by German Research Council (DFG) projects TR18 and GRK 1203.

References

1. G. Mourou, B. Brocklesby, T. Tajima, J. Limpert, Nature Photonics **7**, 258 (2013)
2. A. Pukhov, I. Kostyukov, T. Tückmantel, P. Luu-Thanh, G. Mourou, Euro. Phys. J. Special Topics **223**, 1197 (2014)
3. A. Pukhov, J. Plasma Phys. **61**, 425 (1999)
4. A.J. Kemp, R.E.W. Pfund, J.M. ter Vehn, Phys. Plasmas **11**, 5648 (2004)
5. V.S. Popov, Physics - Uspekhi **47**, 855 (2004)
6. M. Chen, E. Cormier-Michel, C. Geddes, D. Bruhwiler, L. Yu, E. Esarey, C. Schroeder, W. Leemans, J. Computational Phys. **236**, 220 (2013)
7. M.V. Ammosov, N.B. Delone, V.P. Krainov, Sov. Phys. JETP **64**, 1191 (1986)